STUDIA UNIVERSITATIS BABES-BOLYAI, CHEMIA, LIV, 1, 2009

Dedicated to Professor Liviu Literat, at his 80th anniversary

THE INFLUENCE OF SOLID SURFACE ON THE ADSORPTION OF ANTI-C1Q MONOCLONAL ANTIBODY AT ISOELECTRIC pH

IOAN BALEA[a], MARIA TOMOAIA-COTIŞEL[a*], OSSI HOROVITZ[a], GHEORGHE TOMOAIA[b], AURORA MOCANU[a]

ABSTRACT. The effect of solid surface and ionic strength, in a buffer solution at isoelectric pH (5.5), on the surface immobilization, and adsorption process of a mouse monoclonal antibody, type IgG1, anti-C1q, is investigated by atomic force microscopy (AFM). The adsorption is conducted on glass, amino silanized glass, and positively charged modified glass. The AFM images present a monolayer adsorption with a dominant lying flat orientation of the molecules. This suggests that van der Waals interactions and possibly hydrogen bonds between antibody molecules and the solid substrate are the dominant interactions upon electrostatic forces, in conditions of rather low surface charge densities, high ionic strength of buffer solutions, and antibody molecules without a net charge.

Keywords: *anti-C1q monoclonal antibody, adsorption, AFM, ionic strength, surface charge*

INTRODUCTION

Proteins and particularly antibodies are in the focus of interest for investigations by various modern physical methods. Their immobilization in stable adsorption layers on solid surfaces is important in diverse applications, therefore the antibody adsorption has been undertaken on a variety of surfaces, such as mica, silica, glass and gold [1-3], by using different techniques. Among them, atomic force microscopy (AFM) has proved as a versatile technique capable of providing information at nanometer and molecular level, e.g. the structural morphology and the spatial distribution of antibody molecules as well as the antibody layer thickness and roughness on the solid surface [4-11].

[a] *Universitatea Babeş-Bolyai, Facultatea de Chimie şi Inginerie Chimică, Str. Kogălniceanu, Nr. 1, 400048, Cluj-Napoca, Romania, mcotisel@chem.ubbcluj.ro*
[b] *Universitatea de Medicină şi Farmacie, Str. Mosoiu , Nr. 47, 400132, Cluj-Napoca, Romania*

The anti-C1q monoclonal antibody, the object of our present investigation, is a Y-shaped protein molecule, having a molecular weight of 150 KDa and an isoelectric pH of about 5.5. It is known that this antibody recognizes and reacts specifically with the globular heads of the C1q protein, which plays a central role in innate immunity, being involved in the early phase of the classical pathway of the complement system activation [12]. It is also known that the C1q protein is involved in the pathogenesis of a wide range of diseases [13-15], such as Alzheimer`s disease, prionic diseases and lupus erythematosus systemic. Immunohistochemistry uses this monoclonal antibody specific for C1q protein in ELISA [16], RIA (radio immunoassay), Western blotting and flow cytometry methods [17]. For example, ELISA is a solid-phase immunoassay [16] frequently used in immunology, biochemistry, biophysics, medical diagnostics, and other areas of medical science. This immunoassay involves the immobilization of one reactant, such as a specific antibody, on the solid surface usually by adsorption.

Usually in the antibody molecule we distinguish between the *Fab* fragment (antigen-binding fragment), which binds analyte (antigen) with high specificity, and the *Fc* fragment (constant fragment). For immunoassay applications, the control of adsorption and orientation of antibodies on surfaces is necessary to ensure that their active sites (the two “ends” of the Y-shaped molecule) are away from the surface and accessible to bulk solution, i.e. the Fc fragment (the “head” of the molecule) binds to the solid surface.

Here we investigate the effects of various adsorption surfaces and physical factors such as ionic strength over the adsorption process of the anti-C1q monoclonal antibody at the isoelectric point (IEP), where the net charge of the antibody is almost zero (pH = 5.5). We employed AFM to image the morphology of the adsorbed layer and to observe adsorption patterns on a variety of hydrophilic solid surfaces, such as glass, silanized glass and positively charged glass and for ionic strengths of 0.031 and 0.055. AFM is used to evidence the relative changes in the thickness of the antibody adsorbed layers and the possible surface aggregation (i.e. surface clusters).

RESULTS AND DISCUSSION

Ionic strength of buffer solutions. The ionic strength of a solution is defined as a function of the concentrations of all the ions present in a solution and of their charges:

$$J = \frac{1}{2}\sum_i c_i z_i^2$$

where c_i is the molar concentration of ion i (mol dm^{-3}), z_i is the charge number of that ion, and the sum is taken over all ions in the solution. In

order to calculate the ionic strength, a speciation of the buffer solutions had to be made. With use of the Hyperquad simulation and speciation (HySS) program [18], we obtain the distribution of species concentrations versus pH for the 10 mM solution of citric acid and citrates (Fig. 1). If we denote the citric acid $C_6H_8O_7$ as H_3A and its sodium salts by NaH_2A, Na_2HA and Na_3A, the species present in the buffer solutions at different pH = 5.5 are calculated to be about: H_2A^- 10%; HA^{2-} 80%; A^{3-} 10%.

Therefore, for the 10 mM buffer solution at pH = 5.5 the concentrations of the ionic species are: $[H_2A^-]$ = 1 mM; $[HA^{2-}]$ = 8 mM; $[A^{3-}]$ = 1 mM; $[Na^+]$ = 1 + 8·2 + 1·3 = 20 mM. The ionic strength is here:

$$J = \frac{1}{2}\left(1\cdot 1^2 + 8\cdot 2^2 + 1\cdot 3^2 + 20\cdot 1^2\right)\cdot 10^{-3} = 3.1\cdot 10^{-2}\,M$$

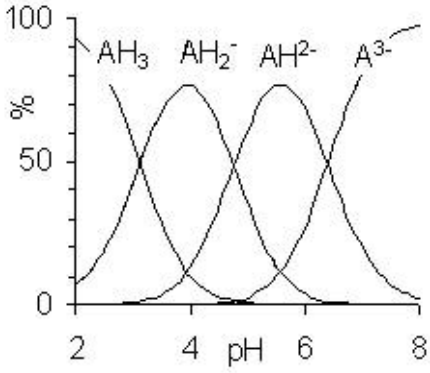

Figure 1. Species distribution versus pH calculated for a 10 mM solution of citric acid (AH_3) pK_{a1}=3.13, pK_{a2} = 4.76, pK_{a3}=6.40 and citrates.

By adding 0.15 M NaCl solution (0.5 mL), J = 0.15, to 2 mL buffer solution, the ionic strength becomes: $J = \frac{2}{2.5}3.1\cdot 10^{-2} + \frac{0.5}{2.5}\cdot 0.15 = 5.48\cdot 10^{-2}\,M$.

Solid surface characteristics. The following surfaces were used for antibody adsorption: freshly cleaned optically polished glass plates, and modified glass (positively charged glass - enriched in Al^{3+} ions, and amino silanized glass). It is known that glass plates in contact with water are negatively charged. The point of zero charge, i.e. the pH at which the surface density of positive charges is equal to the surface density of negative charges, for silica is around pH 2 to 3 [19, 20], that is at higher pH values the solid surface is negatively charged [21]. The same should apply to glass surfaces.

The chemical reactions describing amino silanization are [22]:

- the partial hydrolysis of the aminosilan with traces of water in the solvent (Scheme 1):

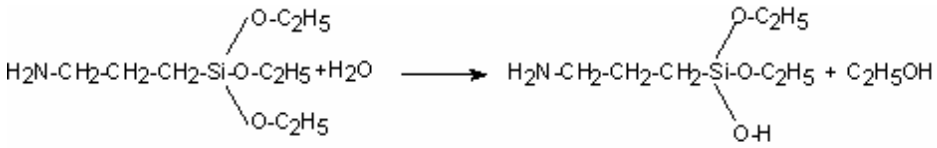

Scheme 1

- the binding on the glass surface (silicate ions) is given in Scheme 2:

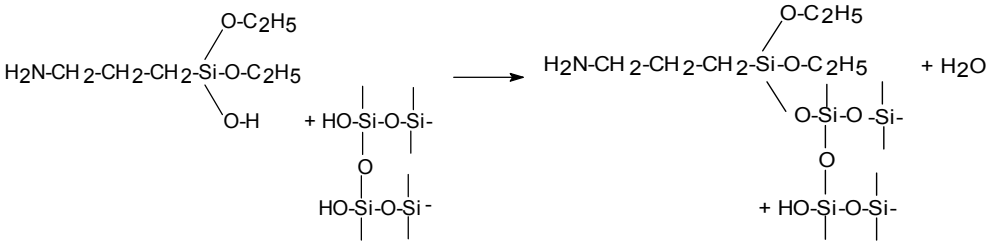

Scheme 2

Surface charge measurements indicated that aminosilanization converts the glass surface from negative to positive potentials at neutral pH values [23]. The equilibrium between protonated amine groups (NH_3^+) and amine group (NH_2) is characterized by the K_a value of the conjugated acid of the amine; this constant can be estimated as being of the order of magnitude of the known value for propylamine [21]: $pK_a \approx 10.2$. That means that for a pH value of 10.2 there are around 50% uncharged $–NH_2$ and 50% protonated $–NH_3^+$ groups. At lower pH values, most of the amine group are protonated, giving a net positive charge to the surface.

As it was shown, only 30 to 50% of silanol groups are grafted during silanization reaction [24], and thus on an aminosilanized glass (or silica) surface, there are likely to be present both amine and silanol (Si-OH) groups.

All the used surfaces are very hydrophilic (contact angle $\theta = 0^o$), except for amino silanized glass surfaces which are poorly wettable. For amino NH_3^+ terminated silane monolayers on silicon, a contact angle between $\theta = 42^o$ for completely ionized NH_3^+ groups (at low pH values) and $\theta = 62^o$ for non ionized NH_2 groups (at high pH values) was reported [25]. The corresponding values for amino silanized glass surfaces should be similar.

Characterization of the adsorbed antibody layers. The differences both in morphology and in the thickness of adsorbed antibody layers might arise from the different orientation of the molecules on the surface, but also from structural modification/deformation of adsorbed protein molecules associated with different electrostatic interactions (attractions or repulsions) between antibody molecules within the antibody layers as well as among the antibody molecules and the solid surface. In order to evidence the influence of different factors on the surface morphology and molecular orientation of the

antibody molecules adsorbed on various solid supports, the height and roughness (RMS) of adsorbed layers obtained from antibody solutions, estimated from AFM images, are presented in Table 1.

Table 1. AFM characterization of anti-C1q antibody layers adsorbed on different solid surfaces at pH = 5.5 (scanned area 0.5 μm x 0.5 μm).

Fig.	J mol/L	Solid surface	Conc. mg/L	Height Å	RMS on area
2	0.031	Silanized glass	2	40-54	1.1
3	0.055	Silanized glass	1.6	40	0.7
4	0.031	Positively charged glass	2	40-53	1.6
5	0.055	Positively charged glass	1.6	40	0.9
6	0.055	Glass	1.6	42	0.7

The antibody adsorption was performed at three bulk antibody concentrations, at about 0.9, 1.6 and 2 mg/L in aqueous buffer solutions. An analysis of AFM images showed that the antibody adsorption reached a steady state saturation of the solid surface within 2 hours at 20 ^{o}C, in substantial agreement with its adsorption carried out for comparison at 17 hours at 4 ^{o}C. This is also in general agreement with data reported for the adsorption of other proteins (e.g. storage protein from aleurone cells of barley) on solid surfaces [26, 27]. Thus, even at low bulk concentration this antibody exhibits a quite high affinity to solid surfaces used.

Typical AFM images of antibody adsorption on *amino silanized glass surface* from a 2 mg/L solution (J = 0.031 M) are given in Fig. 2. For the same surface, but with a 1.6 mg/L antibody solution (J = 0.055 M), AFM images are given in Fig. 3. The main feature of the adsorbed layer is the almost uniform distribution of antibody particles on the silanized glass surface (Figs. 2 and 3; panels: a, b, c, d). The analysis of representative cross section profiles (Fig. 2e and 3e) show that the antibodies films are about 40 to 54 Å high (Table 1). The antibody particles have lateral dimensions typically in the range of 15 to 30 nm.

The anti C1q antibody belongs to the same type IgG1 as the mouse monoclonal antibody, anti-β-hCG [28]. For anti-β-hCG antibody on the basis of the X-ray crystallographic molecular dimensions of 3.8 x 8.5 x 14.2 nm [28-31] are given. For fibrinogen molecules the corresponding data are 4.5 x 4.5 x 47 nm [28, 32-34]. Considering that the size of anti-C1q antibody is close to the anti-β-hCG antibody, it is reasonable to suggest that the observed antibody particles are predominantly monomers. The scan height of about 4 nm for anti-C1q antibody molecules is closed to the short axial length of 3.8 nm of the antibody molecule. This finding reveals that antibody molecules adsorbed in the flat-on orientation with the antibody molecules lying flat on the solid surface. However some particles are larger and could have a certain declivity toward the surface. An almost compact

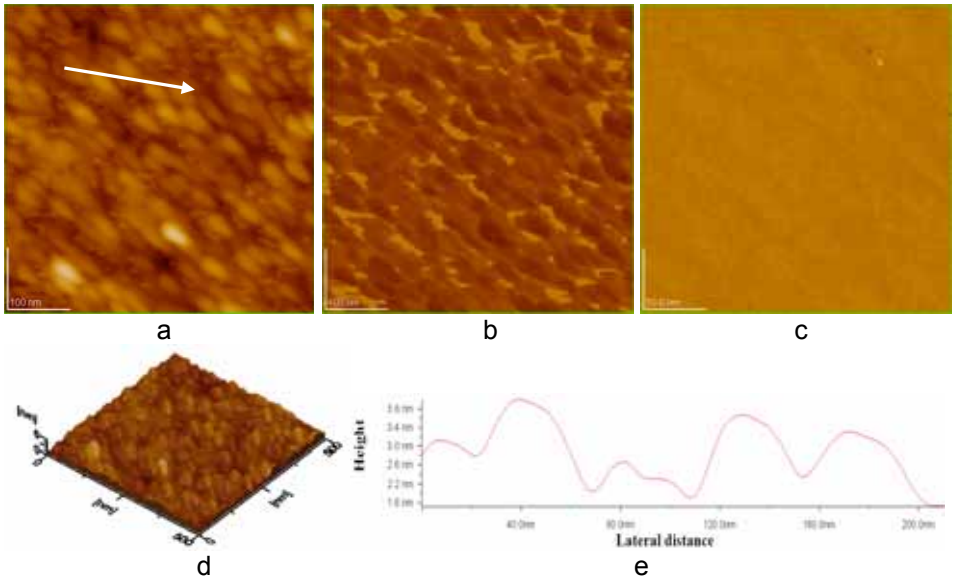

Figure 3. AFM images for antibody adsorbed on silanized glass from 1.6 mg/L antibody solution, J ≈ 0.055: a) 2D – topography; b) phase image; c) amplitude image; d) 3D-topography; e) profile of the cross section along the arrow in fig. (a).

layer of random orientations results, with representative granular structure in substantial agreement with the adsorption of IgG protein on silanized mica surface [35].

In the case of the *positively charged glass surface*, enriched in Al^{3+} ions (Figs. 4 and 5), the observed heights (Table 1) are similar to those for the amino silanized surface, both for 0.031 M and 0.055 M ionic strength, suggesting that antibody molecules form a monolayer of rather "lying flat" molecular orientation.

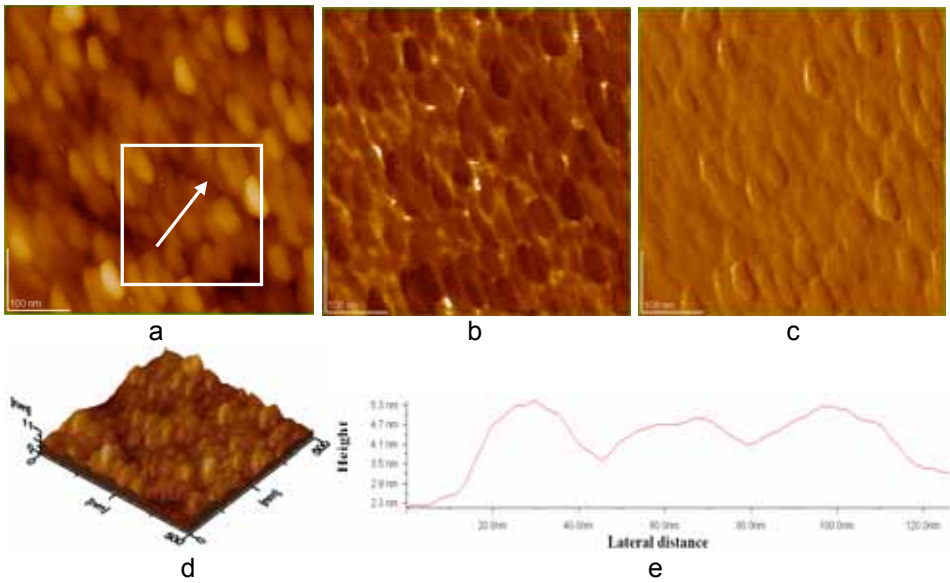

Figure 4. AFM images for antibody adsorbed on glass (positively charged) from 2 mg/L antibody solution, J ≈ 0.031: a) 2D – topography; b) phase image; c) amplitude image; d) 3D-topography; e) profile of the cross section along the arrow in fig. (a).

Generally, it is found that at the isoelectric point, where the net charge of the antibody is zero, the *Fab* fragments will still carry positive charge while the *Fc* fragment will carry negative charge [36-38], and therefore the antibody molecule has a nonzero dipole moment. Physical adsorption is affected by several factors, such as van der Waals interaction, electrostatic interaction, hydrophobic effect, hydrogen bonding, pH values and ionic strength of the solution etc. A Monte Carlo simulation on models of antibody adsorption on charged surface [39] described the orientation of adsorbed antibody molecules as a result from the compromise between electrostatic and van der Waals interactions. The dipole moment of an antibody is an important factor for its orientation on charged surfaces when electrostatic interactions dominate. In this situation, on positively charged

solid surfaces the antibody molecules are oriented preferentially with the negative Fc "head" towards the surface, while on negatively charged surfaces the orientation with the positive Fab ends on the surface is preferred. These orientations are promoted by high surface charge density, high dipole moments of molecules and low solution ionic strength, where electrostatic interactions dominate. At low surface charge density and high solution ionic strength van der Waals interactions dominate, and the antibody molecules have a "lying-flat'' orientation on surfaces.

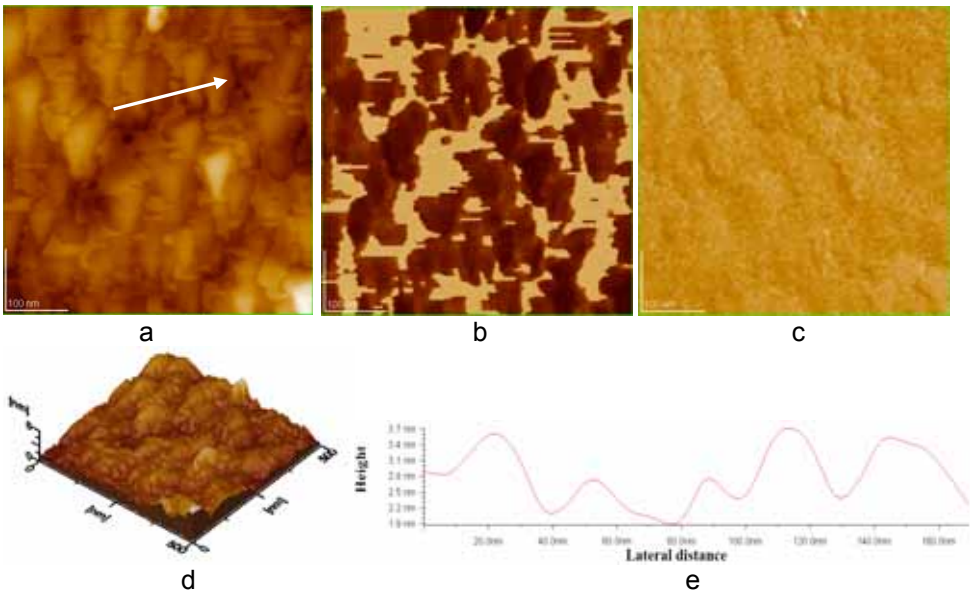

Figure 5. AFM images for antibody adsorbed on glass (positively charged) from 1.6 mg/L antibody solution, J ≈ 0.055: a) 2D – topography; b) phase image; c) amplitude image; d) 3D-topography; e) profile of the cross section along the arrow in fig (a).

Our results suggest that for the rather low positive charge densities on the modified glass surfaces and the quite high ionic strength of the solutions, the flat orientation is predominant. However, for the lower ionic strength (Figs. 2 and 4) both the height of the layers and their roughness (as measured by the RMS values of the adsorbed layers) are somewhat greater than for the higher ionic strength (Figs. 3 and 5) as expected from the above model.

The AFM images for the adsorbed anti-C1q antibody molecules on *glass surface* (Fig. 6), negatively charged, look very similar to the corresponding images for adsorption on positively charged glass and the height is also the same (Table 1). The orientation of the molecules should however be in this case with the Fab ends toward the surface ("head on"), but for the quite

high ionic strength of the buffer solution, the flat orientation given by van der Waals interactions dominates.

The model calculations [39] indicate that the intermolecular antibody-antibody interactions are much less important than antibody–solid surface interactions for the investigated systems, therefore protein–protein interactions do not significantly affect protein orientation even at high surface coverage and multilayer formation is not expected.

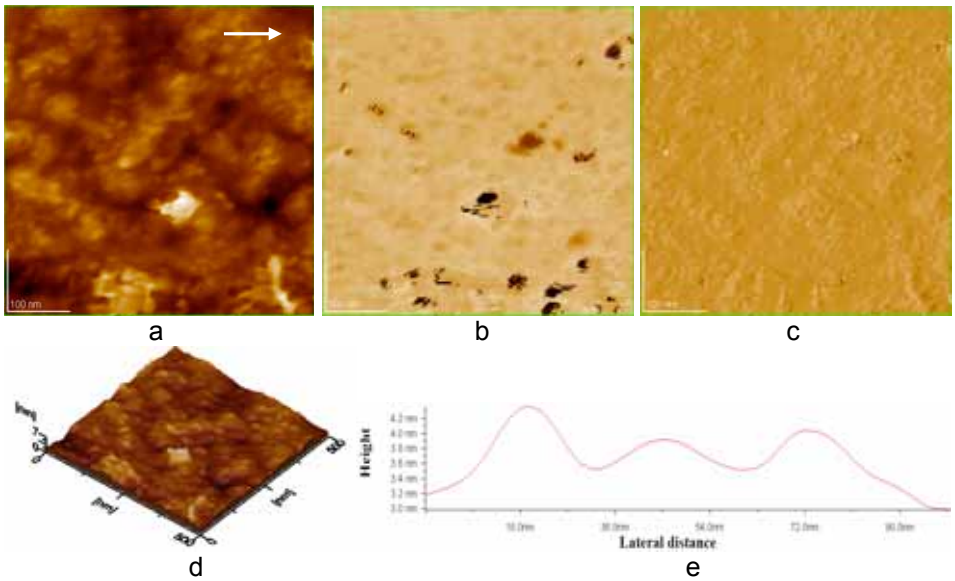

Figure 6. AFM images for antibody adsorbed on glass from 1.6 mg/L antibody solution, J ≈ 0.055: a) 2D – topography; b) phase image; c) amplitude image; d) 3D-topography; e) profile of the cross section along the arrow in fig (a).

CONCLUSIONS

The interpretation of AFM images shows that anti-C1q monoclonal antibody adopts a flat on orientation with an average thickness of about 40 Å, when adsorbed on amino silanized glass, glass negatively charged or glass positively charged for isoelectric pH (about 5.5) of aqueous buffer solution of antibody, for used bulk concentrations of antibody 2 mg/L and 1.6 mg/L and at 0.031 M and 0.055 M ionic strengths. Only antibody monolayers seem to be formed on the used solid surfaces. At this isoelectric pH value, the anti-C1q antibody molecules are without net charge. Due to the uncharged antibody molecules, to the rather low surface charge density, and to the high ionic strength of the solutions screening the electrostatic interactions, these forces are not the dominant factor in controlling the adsorption and orientation of antibody molecules in this case. Van der Waals seems to play

here an important role in determining the orientation of adsorbed antibodies, as well as hydrogen bonding.

Thus, our data suggest that protein-solid surface attractive interactions, more than intermolecular protein-protein forces have a primary importance for molecular orientation within the adsorbed anti-C1q antibody layers. Further, the conformational changes induced in adsorbed anti-C1q antibody molecules due to the attractive interactions with the substrate might cause a distortion of the molecules.

Investigations at other pH values of the solution, where the antibody molecules bear a net positive (lower pH values than the isoelectric pH) or negative (higher pH values) charge will complete the study of the factors making possible the control of the orientation, and conformation of antibodies upon adsorption. This is of outstanding importance for the numerous applications of antibodies in biotechnology and clinical medicine, where the antibody is employed as a molecular recognition element that binds specifically to its antigen with high affinity and is often required to be immobilized on a solid support.

EXPERIMENTAL SECTION

The antibody used in this study was a mouse monoclonal anti-C1q. The antibody was purchased (Cat. No. A201) from Quidel Corporation (San Diego, CA, USA). It was used in 10 mM citric acid / sodium citrate buffer of pH value of 5.5. The ionic strength of the solution was adjusted by adding 150 mM NaCl solution. Three antibody concentrations were prepared, about 0.9, 1.6, 2 mg/L All chemicals used in the present work (citric acid, trisodium citrate, Na_2HPO_4, NaH_2PO_4, NaOH, NaCl) were of analytical reagent grade and used without further purification.

Prior to each adsorption experiment, the glass surface (plates with an area of 2x2 cm^2) was cleaned under known protocol, followed by strong rinsing with deionized water with resistivity bigger than 18 Mohm cm. Then, some clean glass surfaces were further modified as described bellow.

In order to obtain positively charged glass, the glass plates were washed with detergent, rinsed with water and dried. After this, they were washed again with chromic mixture, rinsed with a lot of water, and dried. In the next step, the glasses were immersed in a 2 mM solution of $Al(NO_3)_3$ at 90^o C for 30 min. Afterwards, the glass plates were washed with deionized water and dried.

The silanization was made using aminopropyltriethoxysilane [22, 40, 41] as follows. The glass plates we cleaned as shown above. Later, the glasses we boiled with chromic acid for one hour and cooled slowly to the room temperature. The glass plates were washed extensively with bidistilated water

and dried at 100^{o} C for 1 hour. Then, the glass plates were immersed in a 1 % solution of aminopropilethoxysilan in methanol (freshly prepared) at room temperature for one hour. Further, the glass plates were washed with methanol, treated with ultrasounds in methanol medium and dried for one hour at 100^{o} C.

The antibody coating layers on the solid substrates were prepared by immersing the solid substrate vertically in the antibody aqueous solutions at room temperature for 2 hours or for 17 hours at 4 ^{o}C. After the adsorption (incubation) time, each sample was withdrawn and gently rinsed with deionized water and dried at room temperature, under a beaker and prepared for AFM investigation. As an alternative some samples were dried under a weak but stable nitrogen stream and then immediately subjected to AFM imaging. In the last situation, the drying took less than 0.5 min. As recently mentioned [28], such a short drying process does not provoke the antibody structural modifications or its surface aggregation.

Then, all samples were investigated by AFM in tapping mode, to minimize the force exerted from the scanning tip on the adsorbed antibody layers. The AFM imaging was performed on JEOL 4210 equipment. All measurements were performed in air at room temperature for high lateral image resolution. Standard cantilevers, non-contact conical shaped of silicon nitride coated with aluminum, were used. The sharpened tips were on cantilevers with a resonant frequency in the range of 200 - 300 kHz and with a spring constant of 17.5 N/m. AFM images were collected at a scan angle 0^{o} and at a scan rate of about 1 Hz.

To unravel structural features, the antibody adsorbed layers were visualized from large scan area of 20 x 20 μm^2 to relatively small areas of 1x1 and 0.2 x 0.2 μm^2. AFM observations were repeated on different areas of the same film. The images were obtained from at least five macroscopically separated areas on each sample. All images were processed using the standard procedures for AFM. AFM images consist of multiple scans displaced laterally from each other in y direction with 512 x 512 pixels. All AFM experiments were carried out under ambient laboratory conditions (about 20 ^{o}C) as previously reported [26, 27, 42]. The AFM images on samples prepared in both drying procedures show no observable drying patterns under the experimental working conditions. This study is done under comparable surface packing density, at the same adsorption time (2 hours at room temperature), at quasi saturation of surface with antibody.

ACKNOWLEDGMENTS

This research was realized having financial support from the Scientific research project no. 41-050/2007, within the PN2 Program.

REFERENCES

1. J. P. Gering, L. Quaroni, G. Chumanov, *Journal of Colloid and Interface Science*, **2002**, *252*, 50.
2. Q. Weiping, X. Bin, W. Lei, W. Chunxiao, Y. Danfeng, Y. Fang, Y. Chunwei, W. Yu, *Journal of Colloid and Interface Science*, **1999**, *214*, 16.
3. F. Caruso, E. Rodda, D. N. Furlong, *Journal of Colloid and Interface Science*, **1996**, *178*, 104.
4. N. H. Thomson, *Journal of Microscopy*, **2005**, *217*, 193.
5. A. S. Lea, A. Pungor, V. Hlady, J. D. Andrade, J. N. Herron, E. W. Voss, Jr., *Langmuir*, **1992**, *8*, 68.
6. J. N. Lin, B. Drake, A. S. Lea, P. K. Hansma, J. D. Andrade, *Langmuir*, **1990**, *6*, 509.
7. W. D. Marcus, H. Wang, S. M. Lindsay, M. R. Sierks, *Nanomedicine: Nanotechnology, Biology, and Medicine*, **2008**, *4*, 1.
8. L. S. Shlyakhtenko, B. Yuan, S. Emadi, Y. L. Lyubchenko, M. R. Sierks, *Nanomedicine: Nanotechnology, Biology, and Medicine*, **2007**, *3*, 192.
9. M. Targosz, A. Labuda, P. Czuba, R. Biedron, M. Strus, A. Gamian, J. Marcinkiewicz, M. Szymonski, *Nanomedicine: Nanotechnology, Biology and Medicine*, **2006**, *2*, 82.
10. B. Walivaara, A. Askendal, I. Lundstrom, P. Tengvall, *Journal of Colloid and Interface Science*, **1997**, *187*, 121.
11. R. M. MacCallum, A. C. R. Martin, J. M. Thornton, Journal of Molecular Biology, **1996**, *262*, 732.
12. R. Ghai, P. Waters, L. T. Roumenina, M. Gadjeva, M. S. Kojouharova, K. B. Reid, R. B. Sim, U. Kishore, *Immunobiology*, **2007**, *212*, 253.
13. A. J. Tenner, M. I. Fonseca, *Advances in Experimental Medicine and Biology*, **2006**, *586*, 153.
14. L. Truedsson, A. A. Bengtsson, G. Sturfelt, *Autoimmunity*, **2007**, *40*, 560.
15. H. Zanjani, C. E. Finch, C. Kemper, J. Atkinson, D. McKeel, J. C. Morris, J. L. Price, *Alzheimer Disease & Associated Disorders*, **2005**, *19*, 55.
16. J. E. Butler, L. Ni, R. Nessler, K. S. Joshi, M. Suter, B. Rosenberg, J. Chang, W.R.Brown, L.A. Cantarero, *Journal of Immunological Methods*, **1992**, *150*, 77.
17. E. Potlukova, P. Kralikova, *Scandinavian Journal of Immunology*, **2008**, *67*, 423.
18. L. Alderighi, P. Gans, A. Ienco, D. Peters, A. Sabatini. A. Vacca, *Coordination Chemistry Reviews*, **1999,** *184*, 311.
19. G.A. Parks, *Chemical Reviews*, **1965**, *65*, 177.
20. A. Carré, F. Roger, C. Varinot, *Journal of Colloid and Interface Science,* **1992**, *154*, 174.
21. A. Carré, V. Lacarrière, W. Birch, *Journal of Colloid and Interface Science,* **2003**, *260*, 49
22. J.A. Kiernan, Microscopy Today, **1999**, *99*, 22.
23. E. Metwalli, D. Haines, O. Becker, S. Conzone, C. G. Pantano, *Journal of Colloid and Interface Science,* **2006**, *298*, 825.

24. E.F. Vansant, P. Van der Voort, K.C. Vranken, „Characterization and Chemical Modification of the Silica", in: *Studies in Surface Science and Catalysis*, Vol. *93*, Elsevier, Amsterdam, **1995**.
25. A. Liebmann-Vinson, L. M. Lander, M. D. Foster, W. J. Brittain, E. A. Vogler, C. F. Majkrzak, S. Satija, *Langmuir*, **1996**, *12*, 2256.
26. M. Tomoaia-Cotisel, A. Tomoaia-Cotisel, T. Yupsanis, Gh. Tomoaia, I. Balea, A. Mocanu, Cs. Racz, *Revue Roumaine de Chimie*, **2006**, *51*, 1181.
27. M. Tomoaia-Cotisel, in: M. Zaharescu, E. Burzo, L. Dumitru, I. Kleps, D. Dascalu (Eds.), „Convergence of Micro-Nano-Biotechnologies", Romanian Academy Press, Bucharest, **2006**, pp. 147-161.
28. X. Wang, Y. Wang, H. Xu, H. Shan, J. R. Lu, *Journal of Colloid and Interface Science*, **2008**, *323*, 18.
29. E. W. Silverton, M. A. Navia, D. R. Davies, *Proceedings of the National Academy of Sciences of the USA*, **1977**, *74*, 5140.
30. J. Deisenhofer, *Biochemistry*, **1981**, *20*, 2361.
31. M. Marquart, J. Deisenhofer, R. Huber, W. Palm, *Journal of Molecular Biology*, **1980**, *141*, 369.
32. A. Toscano, M. M. Santore, *Langmuir*, **2006**, *22*, 2588.
33. P. Cacciafesta, A.D.L. Humphris, K. D. Jandt, M. J. Miles, *Langmuir*, **2000**, *16*, 8167.
34. K. L. Marchin, C. L. Berrie, *Langmuir*, **2003**, *19*, 9883.
35. H. X. You and C. R. Lowe, *Journal of Colloid and Interface Science*, **1996**, *182*, 586.
36. J. Buijs, W. Norde, J. W. T. Lichtenbelt, *Langmuir* **1996**, *12*, 1605.
37. J. Buijs, P. A. W. van den Berg, J. W. T. Lichtenbelt, W. Norde, J. Lyklema, *Journal of Colloid and Interface Science*, **1996**, *178*, 594.
38. F. Fogolari, R. Ugolini, H. Molinari, P. Viglino, G. Esposito, *European Journal of Biochemistry*, **2000**, *267*, 4861.
39. J. Zhou, H.-K. Tsao, Y.-J. Sheng, S. Jiang, *Journal of Chemical Physics*, **2004**, *121*, 1050.
40. O. Seitz, M. M. Chehimi, E. Cabet-Deliry, S. Truong, N. Felidj, C. Perruchot, S. J. Greaves, J. F. Watts, *Colloids and Surfaces A: Physicochemical and Engineering Aspects*, **2003**, *218*, 225.
41. J.A. Kiernan, "Histological and Histochemical Methods", 3rd ed. Butterworth-Heinemann, Oxford, **1999**.
42. O. Horovitz, Gh. Tomoaia, A. Mocanu, T. Yupsanis, M. Tomoaia-Cotisel, *Gold Bulletin*, **2007**, *40(4)*, 295.